Theoretical Study of Potential Energy Surface and Thermal Rate Constants for the $C_6H_5 + H_2$ and $C_6H_6 + H$ Reactions

A. M. Mebel,† M. C. Lin,* T. Yu, and K. Morokuma*

Department of Chemistry and the Cherry L. Emerson Center for Scientific Computation, Emory University, Atlanta, Georgia 30322

Received: January 16, 1997; In Final Form: January 23, 1997[⊗]

The potential energy surface for the $C_6H_5-H_2$ system has been calculated with a modified Gaussian-2 method (G2M). The system includes the reactions $C_6H_5 + H_2 \rightleftharpoons C_6H_6 + H$ (1) and $H + C_6H_6 \rightleftharpoons C_6H_7$ (2). The computed molecular parameters and energetics are employed to calculate the thermal rate constants for these reactions. For the direct abstraction reaction (1), the energy barrier was found to be 8.8 kcal/mol at our best G2M(rcc,MP2) level of theory, with the tunneling corrected transition-state-theory rate constant $k_1 = 9.48 \times 10^{-20}T^{2.43} \exp(-3159/T)$ cm^3/(molecule s) covering 300−5000 K. This result is consistent with scattered kinetic data available in the literature. For the addition reaction (2), the barrier was found to be 8.9 kcal/mol. The rate constant calculated by solving the master equation, with tunneling corrections based on the RRKM theory, gave $k_2 = 5.27 \times 10^{-11} \exp(-1605/T)$ cm^3/(molecule s) at the high-pressure limit and $300 \le T \le 1000$ K. In this temperature regime, where most addition kinetics have been measured, the calculated results between 1 and 100 Torr encompass all experimental data. k_2 was found to be strongly pressure dependent above room temperature. Additionally, the effects of isotope substitution and possible secondary reactions on reported experimental data have been discussed.

I. Introduction

C_6H_5 radicals play an important role in hydrocarbon combustion chemistry, especially in relation to soot formation in its incipient stage.[1,2] In studies by the cavity ring-down (CRD) technique, we have measured the absolute rate constants of phenyl reactions with many molecules relevant to hydrocarbon combustion processes.[3−8] Most of these reactions occur with rate constants greater than 10^{-16} cm^3/(molecule s) above room temperature which are amenable with the CRD method. For reactions such as $C_6H_5 + H_2$, we have not yet been able to reliably measure its reaction rates below 600 K, the upper limit of the temperature range employed in our CRD studies due to the detrimental effect of temperature broadening of C_6H_5 absorption.[3−8]

For the $C_6H_5 + H_2 \rightarrow C_6H_6 + H$ reaction (1), there have been kinetic measurements by conventional methods. Fielding and Pritchard[9] measured its rate constant at low temperatures by a relative rate method using the recombination of C_6H_5 radicals as a reference process. Fujii and Asaba,[10] Rao and Skinner,[11] and Kiefer *et al.*[12] estimated the rate constant for the abstraction process by kinetic modeling of the rates of the C_6H_6 decomposition reaction at high temperatures in shock waves. At the latest International Symposium on Combustion, Troe and co-workers[13] reported the Arrhenius expression $k_{H_2} = 6.6 \times 10^{-12}e^{-3970/T}$ cm^3/(molecule s), obtained by UV absorption spectroscopy using shock-heated mixtures of H_2 and various C_6H_5 precursors. In a similar study at low temperatures by FTIR spectrometry, we have also determined the kinetics of the abstraction reaction. Kinetic modeling of the measured C_6H_6 yields in the temperature range 550−650 K gave rise to a preliminary set of data which will be compared with the calculated result later.

For the related $H + C_6H_6 \rightarrow C_6H_7$ addition reaction (2), numerous kinetic measurements have been conducted using several techniques under varying experimental conditions.[14−21] Since the rate constant for the addition process is pressure dependent, these results will be discussed later by comparing with the calculated values at different pressures.

In this investigation, we calculated the thermal rate constants for both of the title reactions, using the potential energy surface data computed with a modified Gaussian-2 method.[22] These theoretical results are compared with the existing kinetic data for both processes summarized above, including the effects of isotope substitutions.

II. Calculation Methods

The geometries of the reactants, products, and transition states have been optimized using two different methods, MP2/6-31G* and the hybrid density functional B3LYP method, i.e., Becke's three-parameter nonlocal-exchange functional[23] with the nonlocal correlation functional of Lee, Yang, and Parr,[24] with the 6-31G** basis set.[25] Vibrational frequencies, calculated at the B3LYP/6-31G** level, have been used for characterization of stationary points and zero-point energy (ZPE) corrections as well as transition-state-theory (TST) and Rice−Ramsperger−Kassel−Markus (RRKM) computations of the rate constants.[26] All the stationary points have been positively identified for minima (number of imaginary frequencies NIMAG = 0) or transition states (NIMAG = 1). All the energies quoted and discussed in the present paper include the ZPE correction.

In order to obtain more reliable energies, we used higher levels of theory including perturbation theory to the fourth order[27] (spin-projected PUMP4), quadratic configuration interaction (QCISD and QCISD(T)) methods,[28] restricted open-shell coupled cluster (RCCSD and RCCSD(T)) methods,[29] and the equation-of-motion ionization potential (EOMIP-CCSD) approach.[30] The most accurate energetics is calculated by the G2M(rcc,MP2) scheme, which is a modification of the Gauss-

† Present address: Institute of Atomic and Molecular Sciences, Academia Sinica, P.O. Box 23-166, Taipei 10764, Taiwan.

* To whom correspondence should be addressed.

⊗ Abstract published in *Advance ACS Abstracts,* April 1, 1997.

S1089-5639(97)00235-1 CCC: $14.00

TABLE 1: Relative Energies (kcal/mol) of Reactants, Products, and Transition States for the $C_6H_5 + H_2 \rightarrow C_6H_6 + H$ Reaction at Various Levels of Theory at the MP2/6-31G(d) Optimized Geometries

	$C_6H_5 + H_2$[a]	$C_6H_6 + H$	**TS1**	C_6H_7	**TS2**
$\langle S^2 \rangle$ (UHF)	1.26	0.75	1.26	1.15	1.33
ZPE[b]					
UHF/6-31G* (0.89)	57.0	60.1			
UMP2/6-31G* (0.95)	61.3	60.0	57.0	66.5	63.4
B3LYP/6-31G** (1)	61.2	63.1	61.8	68.3	64.1
E_{rel} (w B3LYP ZPE)					
UMP2/6-31G**	−231.945 28	−34.7	9.7	−33.3	−2.2
PUMP2/6-31G**	−231.968 02	−20.4	8.3	−32.9	−5.8
PUMP4/6-31G**	−232.053 25	−14.9	9.2	−34.1	−4.7
PUMP4/6-311G**	−232.129 54	−15.0	8.2	−33.8	−6.1
QCISD(T)/6-31G**	−232.055 15	−13.3	11.3	−31.5	−2.1
RCCSD(T)/6-31G**	−232.056 68	−11.9	10.4	−29.8	−1.4
RCCSD(T)/VDZ	-232.071 96	−10.4	12.9	−28.4	+0.3
G2M(rcc,MP2)	−232.256 56[c]	−11.1	8.8	−28.9	−2.2
RCCSD(T)/6-311G**	−232.141 98	−11.8			
G2M(RCC,MP2)	−232.270 38[c]	−10.8			
EOMIP/6-31G**	−232.016 092	−14.1	10.2	−33.7	−2.1
RCCSD/6-31G**	−232.021 029	−11.0	11.3	−30.6	−0.1
QCISD/6-31G**	−232.019 428	−12.9	11.1	−34.3	−2.5
B3LYP//MP2	−232.743 95	−7.2	5.3	−30.1	−4.2
B3LYP//B3LYP	−232.747 79	−4.8	5.0	−28.3	−1.6
experiment		−8.7 ± 0.6[d]			

[a] Total energies are given in hartrees; all other energies given are relative to $C_6H_5 + H_2$. [b] Zero-point energies in kcal/mol. Scaling factor for each approximation is given in parentheses. [c] ZPE is included in the total energy. [d] Computed on the basis of the experimental strengths of the C−H bond in C_6H_6 (ref 35) and the H−H bond in H_2 (ref 36).

ian-2 (G2) approach by Pople and co-workers,[31] and the total energy is calculated as follows:[22]

$$E[\text{G2M(rcc,MP2)}] = E[\text{PUMP4/6-311G(d,p)}] + \Delta E(\text{RCC}) + \Delta E(+3\text{df2p}) + \Delta E(\text{HLC}) + \text{ZPE}$$

where

$$\Delta E(\text{RCC}) = E[\text{RCCSD(T)/6-31G(d,p)}] - E[\text{PUMP4/6-31G(d,p)}]$$

$$\Delta E(+3\text{df2p}) = E[\text{UMP2/6-311+G(3df,2p)}] - E[\text{UMP2/6-311G(d,p)}]$$

$$\Delta E(\text{HLC}) = -4.93n_\beta - 0.19n_\alpha \quad \text{mhartree}$$

where n_α and n_β are the numbers of α and β valence electrons, respectively.

GAUSSIAN 92/DFT[32] and MOLPRO 94[33] programs were employed for the potential energy surface computations. Figure 1 shows optimized geometries of the reactants, products, and transition states. The energies of all species involved calculated at various levels of theory are summarized in Table 1.

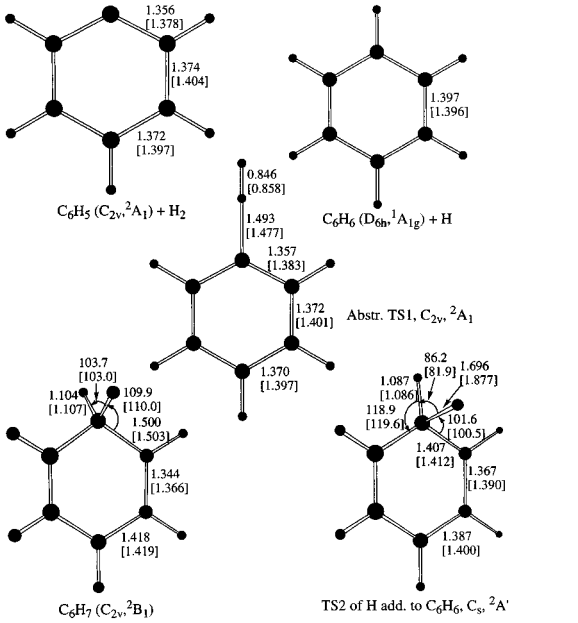

Figure 1. Geometries (bond lengths in angstroms, bond angles in degrees) of the reactants, products, and transition states of the $C_6H_5 + H_2$ and $C_6H_6 + H$ reactions, optimized at the MP2/6-31G* and B3LYP/6-31G** (in brackets) levels of theory.

III. Results

1. Potential Energy Surface of the $C_6H_5 + H_2$ Reaction. The reaction of the phenyl radical with H_2 proceeds by the hydrogen abstraction mechanism to form $C_6H_6 + H$. Another possibility, the insertion of C_6H_5 to molecular hydrogen leading to C_6H_7, will be discussed and ruled out later. **TS1** is the transition state for the abstraction of a hydrogen atom, $C_6H_5 + H_2 \rightarrow C_6H_6 + H$. **TS1** is found to have C_{2v} symmetry; the CHH fragment is collinear. The reaction is exothermic; therefore, the transition state exhibits an early character. The breaking H−H bond is elongated by about 0.1 Å as compared to that in the free H_2 molecule. The C−H distance, 1.48−1.49 Å, in the transition state is still longer by ~0.4 Å than a regular CH bond length. The geometry of the C_6H_5 fragment in **TS1** is almost the same as the geometry of the phenyl radical. It is worth noting that the structure of the CHH fragment in **TS1** is similar to that in the transition state for the $C_2H_3 + H_2 \rightarrow C_2H_4 + H$ abstraction reaction,[34] suggesting that the reaction of the vinyl radical with H_2 can serve as a good model for the corresponding reaction of the phenyl radical. Geometries of C_6H_5, C_6H_6, and **TS1** optimized at the MP2/6-31G* and B3LYP/6-31G** levels are similar; the differences in the bond lengths do not exceed 0.02−0.03 Å.

Before discussing the barrier height, let us consider the reaction exothermicity calculated at various levels of theory, in comparison to the experimental value. The heat of the $C_6H_5 +$

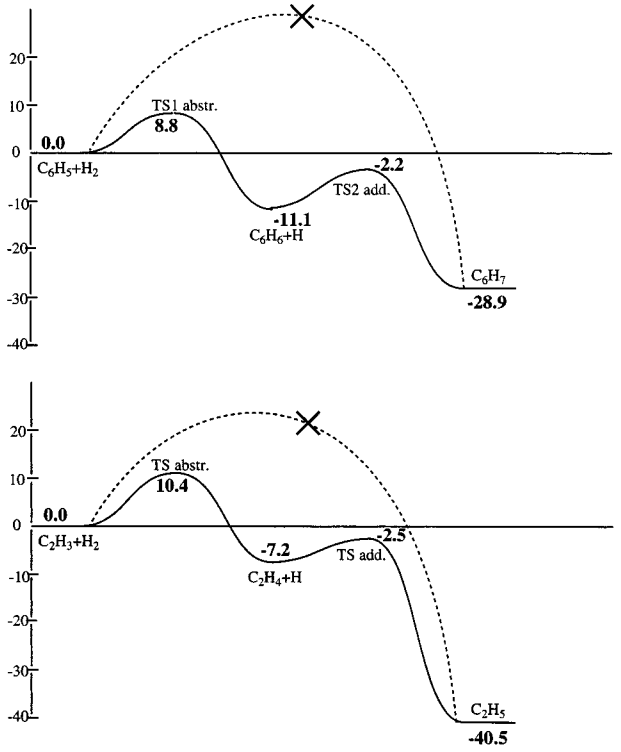

Figure 2. Profiles of potential energy surfaces for the reactions $C_6H_5 + H_2$ and $C_6H_6 + H$ as well as $C_2H_3 + H_2$ and $C_2H_4 + H$, calculated at the G2M(rcc,MP2) level.

$H_2 \rightarrow C_6H_6 + H$ reaction is determined by the strengths of the H−H bond in H_2 and the C−H bond in benzene. The latter, 112.0 ± 0.6 kcal/mol from the recent experiment of Davigo *et al.*,[35] is difficult to reproduce by *ab initio* calculations. The phenyl radical has high spin contamination of the UHF wave function; the $\langle S^2 \rangle$ value is 1.26, much higher than 0.75 for a pure doublet. As a result, the perturbation theory calculations do not give a reliable value for the strength of the C−H bond in C_6H_6. Coupled cluster [RCCSD and RCCSD(T)], quadratic CI [QCISD and QCISD(T)], and EOMIP results with the 6-31G** basis set are more accurate; the calculated C−H bond strength is in the 110.6−113.7 kcal/mol range. On the other hand, all these methods significantly underestimate the H−H bond strength in H_2, giving 99.6 kcal/mol vs the experimental value 103.3 kcal/mol.[36] A balanced treatment of the G2[22,31] or CBS[37] type is needed to better reproduce the experimental heat of the abstraction reaction. For ΔH, the G2M(rcc,MP2) and G2M(RCC,MP2)[22] methods give 11.1 and 10.8 kcal/mol, respectively, only about 2 kcal/mol higher than the experimental value of 8.7 ± 0.6 kcal/mol. The deviation results from the overestimate of ∼3 kcal/mol for the C−H bond strength in C_6H_6 by the G2M methods. The B3LYP/6-31G** approach underestimates ΔH by a few kcal/mol.

At our best level, G2M(rcc,MP2), the barrier for the hydrogen abstraction by C_6H_5 from H_2 is calculated to be 8.8 kcal/mol. This is lower than the barrier for the $C_2H_3 + H_2 \rightarrow C_2H_4 + H$ reaction by 1.6 kcal/mol, calculated earlier by us[34] with a similar method. For the reaction of the vinyl radical with H_2, recent experimental measurements of Knyazev *et al.*[38] showed that our calculated barrier has to be reduced only by 1.4 kcal/mol in order to reach a close agreement between the theoretical and experimental rate constants. A similar level of accuracy can be expected for the calculated barrier height for the $C_6H_5 + H_2$ reaction. Interestingly, recent CASPT2 calculations of Logan and Chen[39] showed that the barrier for hydrogen abstraction from methanol by C_6H_5 is 8.0 kcal/mol.

In Figure 2, we compare potential energy surfaces of the $C_6H_5 + H_2 \rightarrow C_6H_6 + H$ and $C_2H_3 + H_2 \rightarrow C_2H_4 + H$ reactions. The former is somewhat more exothermic than the latter, resulting in the lowering of the abstraction barrier. Hence, one can expect that the phenyl radical is more reactive toward molecular hydrogen than the vinyl radical.

The insertion reaction $C_6H_5 + H_2 \rightarrow C_6H_7$ is symmetry forbidden. Within C_{2v} symmetry, the reactants have $^2A_1$ electronic state, while the electronic state of C_6H_7 is $^2B_1$. We searched for a TS for insertion without symmetry constraints. However, all our calculations converge to either **TS1** for abstraction or **TS2** for the hydrogen addition to C_6H_6, which will be discussed in the next section. Thus, no insertion transition state was located. For the $C_2H_3 + H_2$ reaction, we showed[34] that no TS for insertion leading to C_2H_5 exists. Therefore, we concluded that the reaction of C_6H_5 with H_2 can take place only by the abstraction mechanism, and the only products are benzene and the H atom.

Calculated vibrational frequencies of C_6H_5, C_6H_6, and **TS1** are shown in Table 2. The B3LYP method has been shown to be successful in reproducing experimental frequencies of various molecules and radicals.[22] This is also the case for benzene[40] and the phenyl radical. For the latter, recent infrared absorption spectroscopy measurements[41] showed good agreement between experiment and the calculated B3LYP frequencies. On this basis, we expect the frequencies of the transition state to be reliable. For **TS1**, the imaginary frequency is 905i cm^{-1}, implicating that quantum-mechanical tunneling would affect the reaction rate constant.

2. Potential Energy Surface of the $C_6H_6 + H$ Reaction. The $C_6H_6 + H$ reaction can proceed by two mechanisms: hydrogen abstraction leading to $C_6H_5 + H_2$ and hydrogen addition giving C_6H_7. The first channel has a high barrier, 19.9 kcal/mol according to the G2M(rcc,MP2) calculations. If one corrects the heat of the reaction to the experimental value of 8.7 kcal/mol, the barrier height decreases to 17.5 kcal/mol. This value is still much higher than the calculated barrier for the addition channel, 8.9 kcal/mol at the G2M(rcc,MP2) level. While the $C_6H_6 + H \rightarrow C_6H_5 + H_2$ abstraction reaction is endothermic, the addition channel is exothermic. The computed enthalpy of the reaction at room temperature is 18.9 kcal/mol, which is 2.7 kcal/mol lower than the experimental value of 21.6 kcal/mol.[42] The $C_6H_6 + H \rightarrow C_6H_7$ addition reaction is significantly less exothermic than $C_2H_4 + H \rightarrow C_2H_5$ with ΔH of 33.3 kcal/mol. Accordingly, the calculated barrier for the H atom addition to C_6H_6, 8.9 kcal/mol, is almost twice as high as the barrier for H addition to C_2H_4, 4.7 kcal/mol.[34]

TS2 is the transition state for hydrogen addition. According to its geometry, **TS2** has an early character; the forming C−H bond is long, 1.70−1.88 Å, and the bond alteration in the C_6 ring is small. The MP2 and B3LYP methods give quite different values for the critical C−H bond length. Similarly to the $C_2H_4 + H$ addition TS, the origin of the deviation is the flatness of the potential energy surface. While the C−H distance increases from 1.70 to 1.88 Å, the energy changes by less than 1 kcal/mol. The imaginary frequency in **TS2**, 765i cm^{-1}, is lower than that in the abstraction **TS1**.

3. Rate Constant Calculations. The bimolecular rate constants for the abstraction reactions

$$C_6H_5 + H_2 \rightarrow C_6H_6 + H \quad (1)$$

$$C_6H_5 + D_2 \rightarrow C_6H_5D + D \quad (1')$$

were calculated with the conventional TST including tunneling corrections. Using the molecular and TS data summarized in

TABLE 2: Molecular and Transition-State Parameters of the Reactants, Products and Transition States of the $C_6H_5 + H_2$ and $C_6H_6 + H$ Reactions, Calculated at the B3LYP/6-31G Level**

species	*i*	I_i (10^{-40} g cm^2)	ν_j (cm^{-1})
C_6H_5	*A*	134.8	401, 428, 601, 619, 672, 722, 815, 890, 958, 986,
	B	151.0	988, 1023, 1058, 1081, 1182, 1183, 1313, 1342,
	C	285.7	1473, 1485, 1592, 1646, 3173, 3179, 3192, 3194, 3205
TS1	*A*	150.3	905i, 190, 234, 403, 427, 602, 612, 684, 725, 833,
	B	171.9	896, 960, 960, 969, 994, 1022, 1055, 1063, 1111,
	C	322.2	1186, 1188, 1328, 1346, 1479, 1492, 1603, 1645, 2269, 3174, 3180, 3191, 3195, 3205
TS1	*A*	150.3	664i, 149, 176, 403, 422, 589, 611, 657, 694, 746,
($C_6H_5 + D_2$)	*B*	206.4	776, 832, 902, 954, 959, 993, 1021, 1053, 1089,
	C	356.7	1185, 1188, 1325, 1345, 1472, 1477, 1586, 1645, 1672, 3174, 3180, 3191, 3195, 3205
C_6H_6	*A*	148.0	412, 412, 623, 623, 687, 723, 861, 861, 980, 980,
	B	148.0	1014, 1016, 1023, 1061, 1061, 1175, 1198, 1198,
	C	296.1	1336, 1382, 1513, 1513, 1638, 1638, 3155, 3165, 3165, 3180, 3180, 3191
C_6H_5D	*A*	148.0	391, 412, 616, 618, 620, 717, 791, 861, 872, 938,
	B	158.2	980, 1001, 1006, 1020, 1057, 1105, 1183, 1198,
	C	306.3	1330, 1356, 1484, 1507, 1631, 1633, 2346, 3158, 3165, 3173, 3180, 3188
C_6D_5H	*A*	168.6	358, 373, 521, 597, 600, 626, 670, 719, 799, 829,
	B	179.1	833, 834, 855, 875, 938, 971, 993, 1001, 1195,
	C	347.6	1325, 1371, 1425, 1601, 1606, 2327, 2336, 2345, 2355, 2364, 3173
C_6D_6	*A*	179.1	358, 358, 504, 594, 594, 613, 670, 670, 799, 799,
	B	179.1	826, 826, 838, 847, 875, 875, 966, 983, 1075,
	C	358.1	1324, 1362, 1362, 1595, 1595, 2324, 2336, 2336, 2355, 2355, 2367
TS2	*A*	155.3	765i, 294, 363, 422, 473, 617, 618, 697, 732, 849,
	B	160.8	890, 970, 988, 1002, 1012, 1041, 1054, 1064,
	C	305.1	1179, 1194, 1202, 1349, 1379, 1510, 1520, 1621, 1636, 3177, 3186, 3187, 3201, 3202, 3211
TS2	*A*	160.1	588i, 230, 272, 412, 440, 617, 617, 692, 725, 847,
($C_6H_6 + D$)	*B*	172.4	885, 970, 974, 996, 1009, 1025, 1054, 1064,
	C	311.9	1179, 1194, 1202, 1349, 1379, 1509, 1520, 1621, 1634, 3177, 3186, 3187, 3201, 3202, 3211
TS2	*A*	155.4	753i, 286, 362, 422, 468, 611, 614, 683, 703, 808,
($C_6H_5D + H$)	*B*	170.8	844, 868, 927, 970, 987, 997, 1014, 1052, 1115,
	C	315.1	1187, 1202, 1334, 1360, 1489, 1505, 1616, 1632, 2359, 3179, 3186, 3196, 3202, 3209
TS2	*A*	186.7	752i, 276, 341, 386, 426, 530, 587, 588, 626, 664,
($C_6D_6 + H$)	*B*	191.9	704, 788, 806, 825, 828, 841, 842, 875, 878, 960,
	C	367.4	976, 1073, 1332, 1351, 1376, 1574, 1591, 2341, 2351, 2352, 2369, 2371, 2382
TS2	*A*	191.5	588i, 224, 268, 359, 396, 531, 592, 593, 625, 663,
($C_6D_5H + D$)	*B*	193.4	731, 788, 822, 827, 838, 859, 878, 959, 963, 996,
	C	364.1	999, 1186, 1341, 1357, 1430, 1584, 1592, 2342, 2351, 2362, 2372, 2379, 3193
TS2	*A*	191.7	582i, 223, 268, 359, 391, 525, 587, 588, 618, 663,
($C_6D_6 + D$)	*B*	203.6	691, 786, 787, 822, 828, 829, 841, 875, 878, 956,
	C	374.1	976, 1073, 1332, 1349, 1376, 1574, 1588, 2341, 2351, 2352, 2369, 2371, 2382
C_6H_7	*A*	158.4	177, 381, 525, 566, 593, 638, 722, 770, 875, 937,
	B	161.4	963, 972, 973, 993, 997, 1120, 1175, 1179, 1203,
	C	314.7	1320, 1372, 1426, 1448, 1466, 1559, 1625, 2919, 2928, 3167, 3169, 3187, 3188, 3210
$C_6H_5D_2$	*A*	160.9	159, 378, 492, 555, 591, 635, 695, 757, 798, 850,
	B	179.2	853, 890, 968, 975, 985, 996, 1071, 1098, 1148,
	C	330.0	1205,1277, 1343, 1406, 1463, 1555, 1618, 2129, 2156, 3166, 3168, 3186, 3187, 3209
C_6H_6D	*A*	159.5	168, 380, 505, 561, 592, 637, 707, 763, 837, 851,
	B	170.4	889, 966, 975, 991, 997, 1049, 1123, 1175, 1202,
	C	322.5	1294, 1312, 1357, 1413, 1464, 1556, 1620, 2143, 2921, 3166, 3168, 3186, 3187, 3209
C_6D_6H	*A*	191.3	155, 337, 442, 474, 544, 556, 569, 626, 759, 760,
	B	191.7	771, 804, 840, 848, 850, 857, 912, 960, 1013,
	C	375.5	1138, 1269, 1278, 1290, 1355, 1478, 1577, 2144, 2333, 2334, 2356, 2360, 2377, 2923
C_6D_7	*A*	193.0	147, 336, 429, 474, 539, 549, 568, 625, 759, 759,
	B	200.4	762, 769, 828, 838, 850, 857, 875, 895, 956,
	C	383.3	1070, 1072, 1239, 1269, 1325, 1476, 1575, 2130, 2157, 2333, 2334, 2356, 2360, 2377

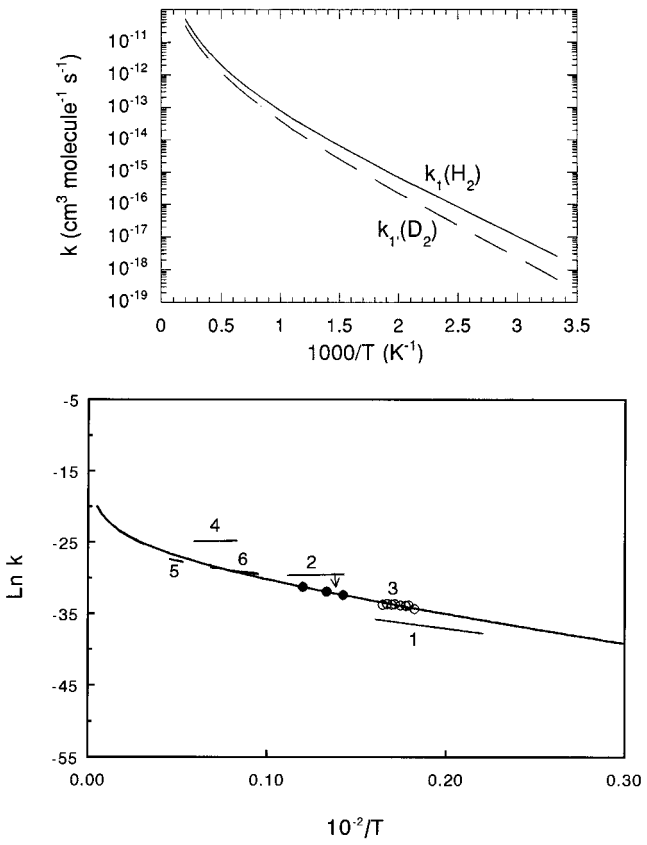

Figure 3. (a, top) Arrhenius plots of rate constants k_1 and k_1' for the abstraction reactions $C_6H_5 + H_2$ and $C_6H_5 + D_2$, respectively. (b, bottom) Comparison of experimental rate constants for the abstraction reaction $C_6H_5 + H_2 \rightarrow C_6H_6 + H$ with the calculated one. Experimental data: (1) ref 9; (2) upper limit, ref 20; (3) ref 45; (4) ref 10; (5) ref 12; (6) ref 13; see text for explanation. Long curve: theory.

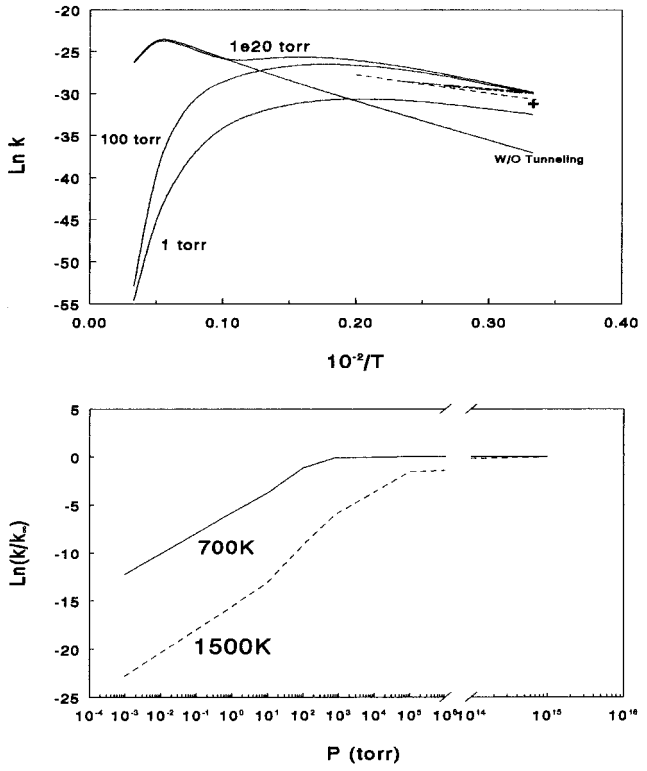

Figure 4. Rate constants for the reaction $C_6H_6 + H \rightarrow C_6H_7$ calculated for various pressures on the basis of the RRKM theory with tunneling corrections. (a, top) Temperature dependence: curves are calculated values for the indicated pressure. (− - - −) ref 18; (− −) ref 17; (- - -) ref 20; (+) ref 46. (b, bottom) Pressure dependence.

Tables 1 and 2, we obtained the following rate expressions for the temperature range 300−5000 K in units of cm^3/(molecule s):

$$k_1 = 9.48 \times 10^{-20} T^{2.43} \exp(-3159/T)$$

$$k_{1'} = 8.85 \times 10^{-20} T^{2.40} \exp(-3570/T)$$

These results are graphically presented in Figure 3a,b. The result of the H_2 reaction will be compared with experimental data later.

For the addition process, a variety of isotopically labeled reactions have been calculated for comparison with experiments:

$$H + C_6H_6 \rightarrow C_6H_7^{\dagger} \xrightarrow{+M} C_6H_7$$

$$D + C_6H_6 \rightarrow C_6H_6D^{\dagger} \rightarrow C_6H_5D + H$$

$$\xrightarrow{+M} C_6H_6D$$

$$H + C_6D_6 \rightarrow C_6D_6H^{\dagger} \rightarrow C_6D_5H + D$$

$$\xrightarrow{+M} C_6D_6H$$

$$D + C_6D_6 \rightarrow C_6D_7^{\dagger} \xrightarrow{+M} C_6D_7$$

where "†" represents vibrational excitation and M denotes a third body which collisionally deactivates the excited adducts.

Because of the existence of well-defined TS's in these reactions, we carried out conventional RRKM calculations by solving the individual master equations using the steady-state approach of Diau and Lin[43] for tunneling corrections.

The computed rate constant for $H + C_6H_6 \rightarrow C_6H_7$ as a function of temperature is shown in Figure 4a for several pressures, and the effect of pressure for 700 and 1500 K is illustrated in Figure 4b.

For isotopically labeled addition reactions, Timmons and coworkers[17] reported in 1973 both absolute and relative (k_H/k_D) values of their rate constants obtained under H and D excess conditions. In Figure 5, we present the calculated k_H/k_D ratios for the reaction pairs $H + C_6H_6/C_6D_6$ and $D + C_6H_6/C_6D_6$ as functions of temperature at 1 Torr pressure, for which the experimental study was performed. A comparison of theory and experiment will be made later.

At high pressures, the theoretical rate constants for the various isotopic combinations can be summarized as follows in units of cm^3/(molecule s) for the 300−1000 K temperature range:

$$k_{H+C_6H_6} = 5.27 \times 10^{-11} \exp(-1605/T)$$

$$k_{D+C_6H_6} = 1.29 \times 10^{-11} \exp(-2574/T)$$

$$k_{H+C_6D_6} = 1.89 \times 10^{-11} \exp(-2234/T)$$

$$k_{D+C_6D_6} = 2.97 \times 10^{-11} \exp(-2540/T)$$

IV. Discussion

1. $C_6H_5 + H_2$ Reaction. In Figure 3b, we compare the calculated rate constant for the abstraction reaction with experimental data. Fielding and Pritchard[9] measured the rate of C_6H_6 formation relative to that of $C_{12}H_{10}$ (biphenyl) produced by the recombination of phenyl radicals in the photolysis of

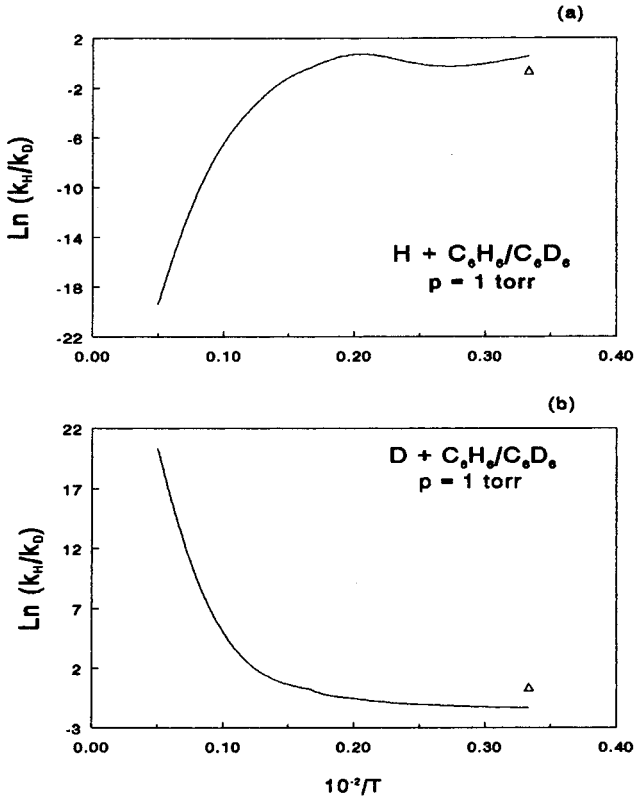

Figure 5. Comparison of the calculated k_H/k_D ratios with the measured values by Timmons and co-workers (ref 17) for (a) H + C_6H_6 and C_6D_6 and (b) D + C_6H_6 and C_6D_6.

biphenyl mercury in the presence of an excess amount of H_2 at $453 < T < 623$ K. The combination of their relative rate constant, $k_1/k_r^{1/2} = 1.2 \times 10^{-8}e^{-3270/T}$ [cm^3/(molecule s)]$^{1/2}$ with the recombination rate constant recently determined by Park and Lin,[44]

$$k_r = 2.3 \times 10^{-11}e^{-56/T} \quad \text{cm}^3/(\text{molecule s})$$

gives rise to

$$k_r = 5.8 \times 10^{-14}e^{-3300/T} \quad \text{cm}^3/(\text{molecule s})$$

The result, labeled as line 1, is lower than our predicted value within their temperature range studied as indicated in Figure 3b.

Recently, we measured k_1 in a similar temperature range by pyrolyzing mixtures of C_6H_5NO and H_2 with and without added NO by FTIR spectrometry.[45] From the rate of formation of C_6H_6 and the decay of C_6H_5NO, we kinetically modeled the rate constant for the abstraction reaction. Our preliminary data, included in the figure by open circles, agree closely with the predicted value. We have also carried out a parallel study of the reaction with the pulsed laser photolysis/mass spectrometry system[44] employing $C_6H_5COCH_3$ as the phenyl source. The result of this preliminary study, given by filled circles in the figure, also agrees quantitatively with the predicted value.

In a study at higher temperatures with a shock tube, Troe and co-workers[13] measured k_1 by UV absorption. Their result, presented in Figure 3b by line 6, also agrees with the computed result. In the same figure, we also compare the high-temperature value of Asaba and Fujii[10] (line 4) from their kinetically modeled rate constant for the reverse H + $C_6H_6 \rightarrow C_6H_5 + H_2$ reaction. In converting the reverse rate constant, we used the equilibrium constant for $C_6H_5 + H_2 = C_6H_6 + H$, $K_{eq} = 9.20 \times 10^{-5}T^{0.636}$ exp(5073/T), based on the theoretical molecular parameters and the experimental exothermicity, 8.7 kcal/mol at 0 K.

In a similar study on the C_6H_6 decomposition reaction, Kiefer *et al.*[12] arrived at the following expression for the rate constant of the H + $C_6H_6 \rightarrow H_2 + C_6H_5$ reaction: $k_{-1} = 4.2 \times 10^{-10}$ exp(−8052/T)cm^3/(molecule s). Combination of this result with the equilibrium constant gives $k_1 = 6.9 \times 10^{-12}$ exp(−3553/T) cm^3/(molecule s). As shown in Figure 3b, the result that is represented by line 5 appears to be in close agreement with our predicted value. We have also included the result estimated with the H + C_6H_6 abstraction reaction, $k_{-1} = 5.0 \times 10^{-12}$ exp(−4076/T) cm^3/(molecule s), by Nicovich and Ravishankara[20] on the basis of their observed H atom decay kinetics above 650 K, assuming no activation energy for the forward $C_6H_5 + H_2$ reaction (line 2). The deviation of these converted estimates from our predicted value, except that of Kiefer et al.,[12] is generally quite large and unreliable.

In Appendix A, we have illustrated that, under the experimental conditions employed by Nicovich and Ravishankara,[20] the H + C_6H_6 abstraction reaction is too slow to be measured because of its large endothermicity (8.7 kcal/mol) and the existence of the reaction barrier for its reverse process, 8.8 kcal/mol. The observed H atom decay rates at all temperatures of their study may be affected by secondary reactions involving the radical and molecular products from the H + C_6H_6 addition reaction.

2. H + C_6H_6 Addition Reaction. The computed rate constant for the addition process

$$H + C_6H_6 \rightarrow C_6H_7 \qquad (2)$$

is presented in Figures 4a,b to illustrate the effects of temperature and pressure. In Figure 4a, the results obtained for 1, 100, and 10^{20} Torr are plotted as functions of temperature. All reported experimental values, typically determined between 1 and 100 Torr, lie within the theoretical values computed with tunneling corrections. To demonstrate the effect of tunneling, we display the curve obtained at 10^{20} Torr without correction. A similar calculation with the conventional TST equation for the addition process at $T < 1000$ K without tunneling correction gave essentially the same as that obtained by solving the master equation. Figure 4b depicts the effect of pressure on k_2 for the two temperatures, 700 and 1500 K, with tunneling corrections. The result reveals the strong dependency on pressure above 1000 K. For practical applications, we recommend the following expression for the addition reaction at 1 atm He covering 700−3000 K:

$$k_2 = 3.1 \times 10^{144}T^{-45.9}\exp(-41165/T) \quad \text{cm}^3/(\text{molecule s})$$

In order to compare the theoretical results with the k_H/k_D ratios reported by Timmons and co-workers[17] for the reaction pairs H + C_6H_6/C_6D_6 and D + C_6H_6/C_6D_6, additional frequency and RRKM calculations were carried out. The predicted k_H/k_D for these reaction pairs at 300 K and 1 Torr pressure, as shown in Figure 5, differ noticeably from the experimental results obtained under [H] or [D] excess conditions. In the experiment by Timmons and co-workers,[17] who measured the disappearance of C_6H_6 or C_6D_6 by mass spectrometry, the [atom]/[benzene] ratios employed were typically in the range 10−24. Under these conditions, many secondary reactions involving the atomic species and radical or molecular adducts including isotopic exchanges may take place as was recognized by these authors. In the H + C_6H_6 reaction, for example, the following reactions may occur:

$$H + C_6H_6 \rightleftharpoons C_6H_7 \text{ (cyclohexadienyl)}$$

$$H + C_6H_7 \rightarrow H_2 + C_6H_6$$

$$H + C_6H_7 \rightarrow C_6H_8 \text{ (cyclohexadiene)}$$

$$H + C_6H_8 \rightleftharpoons C_6H_9 \text{ (cyclohexanyl)}$$

$$H + C_6H_9 \rightarrow H_2 + C_6H_8, \text{ etc.}$$

These reactions, as illustrated in Appendix B, significantly alter the decay kinetics of C_6H_6 or H atoms, depending on which reactant was monitored in the individual experiments.

For the k_H/k_D ratio determined for the $H + C_6H_6$ and $H + C_6D_6$ reaction pair, the measured rate of C_6H_6 decay in the presence of an excess amount of H is expected to be contaminated to a lesser extent by the secondary reactions under low-pressure conditions than that of C_6D_6 decay, because the latter system can undergo additional consumption reactions by isotopic exchanges:

$$H + C_6D_6 \rightarrow C_6D_6H^{\dagger} \rightarrow C_6D_5H + D$$

$$H + C_6D_6H \rightarrow C_6D_5H + HD, \text{ etc.}$$

These additional side reactions will result in a larger k_D than theoretically expected. The calculated $k_H/k_D = 1.74$ at 300 K and 1 Torr pressure is thus much greater than the reported values, 0.55 ± 0.04.[17] Similarly, the theoretical value $k_H/k_D = 0.116$ is considerably smaller than the experimental result of 1.46 ± 0.03 for the reaction pair $D + C_6H_6$ and $D + C_6D_6$, in which additional isotopic exchange processes apparently led to a much larger k_H and thus the expected reversal of the first reaction pair. These isotopic exchange reactions are also expected to become faster at higher temperatures, at which the rate constants for the $H + C_6H_6$ and $D + C_6D_6$ reactions decrease dramatically due to the rapid increase in their reverse rates with temperature (see Figure 4a for 1 Torr pressure). The combined effects result in the predicted sharp drop of k_H/k_D in Figure 5a and the concomitant sharp increase in k_H/k_D in Figure 5b at high temperatures.

The large deviation between our predicted and the reported k_H/k_D ratios by Timmons and co-workers[17] resulted from a poor choice of the experimental method rather than the poor state of the theory.

V. Conclusions

In this study, we have theoretically investigated the potential energy surface of the $C_6H_5 + H_2$ system. The molecular parameters and energies computed for the reactions $C_6H_5 + H_2 \rightarrow C_6H_6 + H$ and $H + C_6H_6 \rightarrow C_6H_7$ have been employed to calculate their rate constants with tunneling corrections using TST and RRKM theories, respectively. The predicted rate constants agree reasonably well with literature values.

Our calculated kinetic isotope effects, expressed in terms of the rate constant ratios k_H/k_D for the reaction pairs $H + C_6H_6/C_6D_6$ and $D + C_6H_6/C_6D_6$ deviate significantly from reported values. This large discrepancy, however, can be readily accounted for by the presence of secondary reactions whose effects grow worse for $H + C_6D_6$ and $D + C_6H_6$, in which additional isotopic exchange processes accelerate the decay rates of C_6D_6 and C_6H_6 measured mass spectrometrically.

Acknowledgment. The authors are thankful to the Cherry L. Emerson Center for Scientific Computation for the use of various programs and computing facilities. A.M.M., M.C.L., and T.Y. acknowledge the support received from the Department of Energy, Office of Basic Energy Sciences, Division of Chemical Sciences, through Contract DE-FGO5-91ER14191. A part of the calculation has been performed on the supercomputer Cray C90 in the Pittsburgh Supercomputing Center through Grant CHE940026P.

Appendix A. Modeling of H Atom Decay Rates under Nicovich and Ravishankara's Conditions

Nicovich and Ravishankara[20] measured the decay of H atoms by atomic resonance fluorescence under $[C_6H_6] >> [H]$ conditions with $[H] = 1 \times 10^{10}-5 \times 10^{11}$ molecules cm^{-3}. We attempted to model the effect of secondary reactions on H atom decays using the mechanism summarized in Table 3. The results of our modeling, using the conditions given in their Figure 2 and $[H] = 1 \times 10^{11}$ molecules cm^{-3} with one secondary reaction (3) and with the full mechanism given in Table 3, are presented in Figure 6a and b, respectively. At 415 K, the calculated pseudo-first-order decay constants are 88 and

TABLE 3: Mechanism for the $H + C_6H_6$ Reaction[a]

reaction	*A*	*B*	*C*	remarks
1. $H + C_6H_6 = H_2 + C_6H_5$	1.0×10^{-15}	1.80	8230	this work
2. $H + C_6H_6 \rightarrow C_6H_7$	6.7×10^{-11}	0.0	2164	*b*
3. $C_6H_7 \rightarrow C_6H_6 + H$	1.3×10^{16}	0.0	16710	*b*
4. $H + C_6H_7 \rightarrow H_2 + C_6H_6$	1.0×10^{-11}	0.0	0	*c*
5. $H + C_6H_7 \rightarrow C_6H_8$	1.2×10^{-10}	0.0	0	*c*
6. $H + C_6H_8 \rightarrow C_6H_9$	2.2×10^{-12}	0.0	0	*c*
7. $H + C_6H_9 \rightarrow C_6H_8 + H_2$	1.0×10^{-11}	0.0	0	*c*
8. $H + C_6H_9 \rightarrow C_6H_{10}$	1.2×10^{-10}	0.0	0	*c*

[a] The rate constants are given by $k = AT^B e^{-C/T}$ in units of cm^3, molecule, and s. [b] k_2 is pressure-dependent; the value is given for 100 Torr of Ar (ref 20). [c] Assumed.

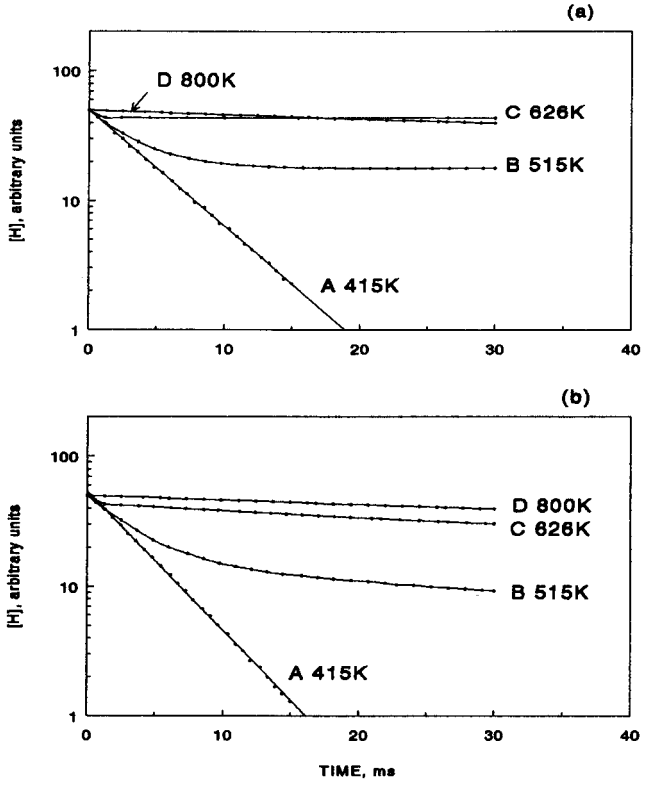

Figure 6. Kinetic modeling of decays of H atoms at various temperatures. Reactant concentrations: $[H] = 1 \times 10^{11}$ atoms cm^3 and $[C_6H_6] = 8.0 \times 10^{14}$ molecules cm^3 diluted to 100 Torr with Ar. (a) Result of modeling with reactions 1−3 given in Table 3. (b) Result of modeling with the full mechanism given in Table 3.

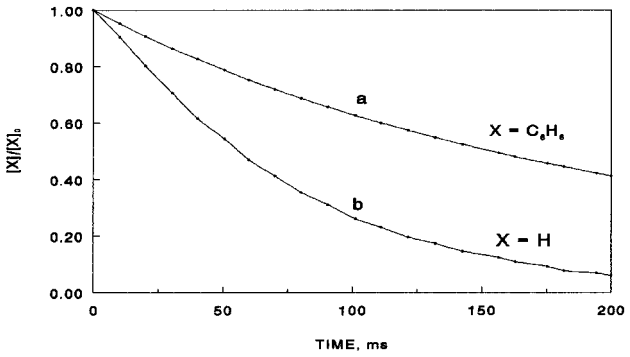

Figure 7. Kinetic modeling of decays of H atoms and C_6H_6 at 300 K at 0.25 Torr pressure. (a) $[H]/[C_6H_6] = 15$. (b) $[C_6H_6]/[H] = 15$ diluted with He to 0.25 Torr.

107 s^{-1}, respectively, with the partial and full mechanisms. This suggests the noticeable (18%) effect of the secondary reactions even under the $[C_6H_6]/[H] = 1 \times 10^3$ condition. At 515 and 626 K, the differences in H decays predicted by both mechanisms are still evident. At 800 K, the difference disappears; both mechanisms predict a decay constant of 4 s^{-1}, because of the domination of reaction 3.

This and other modeling results[47] suggest that the nonnegligible effect of side reactions should be carefully examined and corrected even under pseudo-first-order conditions.

Appendix B. Modeling of H Atom and C_6H_6 Decay Rates under Timmons' Conditions

Timmons and co-workers[17] studied the kinetics of reaction 2 under H atom excess conditions by mass spectrometry using $[H]/[C_6H_6] = 10-24$. We modeled the rates of H-atom and C_6H_6 decay at room temperature at which the effects of isotope substitutions were studied by employing D for H and C_6D_6 for C_6H_6, as mentioned in the text.

The result of our modeling, using the mechanism given in Table 3, is presented in Figure 7 with $[H]/[C_6H_6] = 15$; the pseudo-first-order decay constant for C_6H_6 was calculated to be 2 s^{-1}, whereas with $[C_6H_6]/[H] = 15$ the decay constant for H was found to be a factor of 3 higher, 6 s^{-1}. Theoretically, the two decay rates should be equal if the side reactions are insignificant. The much slower decay of C_6H_6 calculated for their experimental conditions resulted from the regeneration of C_6H_6 by the $H + C_6H_7$ reaction which is significant when an excess amount of H atoms is present.

On account of the presence of various secondary reactions and possible isotopic exchange processes (as mentioned in the text, but not included in Table 3), the results of k_H/k_D reported by Timmons and co-workers[17] should not be associated with the individual elementary H (D) + C_6H_6 (C_6D_6) processes.

References and Notes

(1) Bittner, J. D.; Howard, J. B. *Proceedings of the 18th International Symposium on Combustion*; The Combustion Institute: Pittsburgh, PA, 1981; p 1105.
(2) Glassman, I. *Combustion*, 2nd ed.; Academic Press: New York, 1987.
(3) Yu, T.; Lin, M. C. *J. Am. Chem. Soc.* **1993**, *115*, 4371.
(4) Lin, M. C.; Yu, T. *Int. J. Chem. Kinet.* **1993**, *25*, 875.
(5) Yu, T.; Lin, M. C. *J. Phys. Chem.* **1994**, *98*, 2105.
(6) Yu, T.; Lin, M. C.; Melius, C. F. *Int. J. Chem. Kinet.* **1994**, *26*, 1095.
(7) Yu, T.; Lin, M. C. *Combust. Flame* **1995**, *100*, 169.
(8) Yu, T.; Lin, M. C. *J. Phys. Chem.* **1995**, *99*, 8599.
(9) Fielding, W.; Pritchard, H. O. *J. Phys. Chem.* **1962**, *66*, 821.
(10) Asaba, T.; Fujii, T. *Proc. Int. Shock Tube Symp.* **1971**, *8*, 1.
(11) Rao, V. S.; Skinner, G. B. *J. Phys. Chem.* **1984**, *88*, 5990.
(12) Kiefer, J. H.; Mizerka, L. J.; Patel, M. R.; Wei, H. C. *J. Phys. Chem.* **1985**, *89*, 2013.
(13) Heckmann, E.; Hippler, H.; Troe, J. Presented at the 26th Symposium (International) on Combustion, Naples, Italy, July 28−Aug 2, 1996.
(14) Allen, P. E. M.; Melville, H. W.; Robb, F. R. S.; Robb, J. C. *Proc. R. Soc. London, A* **1953**, *218*, 311.
(15) Sauer, M. C., Jr.; Mani, I. *J. Phys. Chem.* **1970**, *74*, 59.
(16) Knutti, R.; Buhler, R. E. *Chimica* **1972**, *26*, 624.
(17) Kim, P.; Lee, J. H.; Bonanno, R. J.; Timmons, R. B. *J. Chem. Phys.* **1973**, *59*, 4593.
(18) Gordon, E. B.; Ivanov, B. I.; Perminov, A. P.; Balalaev, V. E. *Chem. Phys.* **1978**, *35*, 79.
(19) Hoyermann, K.; Preuss, A. W.; Wagner, H. Gg. *Ber. Bunsen-Ges. Phys. Chem.* **1975**, *79*, 156.
(20) Nicovich, J. M.; Ravishankara, A. R. *J. Phys. Chem.* **1984**, *88*, 2534.
(21) Sauer, M. C., Jr.; Ward, B. *J. Phys. Chem.* **1967**, *71*, 3171.
(22) Mebel, A. M.; Morokuma, K.; Lin, M. C. *J. Chem. Phys.* **1995**, *103*, 7414.
(23) (a) Becke, A. D. *J. Chem. Phys.* **1993**, *98*, 5648. (b) *J. Chem. Phys.* **1992**, *96*, 2155. (c) *J. Chem. Phys.* **1992**, *97*, 9173.
(24) Lee, C.; Yang, W.; Parr, R. G. *Phys. Rev.* **1988**, *B37*, 785.
(25) Hehre, W. J.; Ditchfield, R.; Pople, J. A. *J. Chem. Phys.* **1972**, *56*, 2257.
(26) Laidler, K. J. *Chemical Kinetics*, 3rd ed., Harper and Row: New York, 1987.
(27) Hehre, W.; Radom, L.; Schleyer, P. v. R.; Pople, J. A. *Ab Initio Molecular Orbital Theory*; Wiley: New York, 1986.
(28) Pople, J. A.; Head-Gordon, M.; Raghavachari, K. *J. Chem. Phys.* **1987**, *87*, 5968.
(29) (a) Purvis, G. D.; Bartlett, R. J. *J. Chem. Phys.* **1982**, *76*, 1910. (b) Hampel, C.; Peterson, K. A.; Werner, H.-J. *Chem. Phys. Lett.* **1992**, *190*, 1. (c) Knowles, P. J.; Hampel, C.; Werner, H.-J. *J. Chem. Phys.* **1994**, *99*, 5219. (d) Deegan, M. J. O.; Knowles, P. J. *Chem. Phys. Lett.* **1994**, *227*, 321.
(30) Stanton, J. F.; Gauss, J. *J. Chem. Phys.* **1994**, *101*, 8938.
(31) (a) Curtiss, L. A.; Raghavachari, K.; Trucks, G. W.; Pople, J. A. *J. Chem. Phys.* **1991**, *94*, 7221. (b) Pople, J. A.; Head-Gordon, M.; Fox, D. J.; Raghavachari, K.; Curtiss, L. A. *J. Chem. Phys.* **1989**, *90*, 5622. (c) Curtiss, L. A.; Jones, C.; Trucks, G. W.; Raghavachari, K.; Pople, J. A. *J. Chem. Phys.* **1990**, *93*, 2537.
(32) Frisch, M. J.; Trucks, G. W.; Head-Gordon, M.; Gill, P. M. W.; Wong, M. W.; Foresman, J. B.; Johnson, B. G.; Schlegel, H. B.; Robb, M. A.; Replogle, E. S.; Gomperts, R.; Andres, J. L.; Raghavachari, K.; Binkley, J. S.; Gonzales, C.; Martin, R. L.; Fox, D. J.; DeFrees, D. J.; Baker, J.; Stewart, J. J. P.; Pople, J. A. *GAUSSIAN 92/DFT*; Gaussian, Inc., Pittsburgh, PA, 1993.
(33) MOLPRO is an *ab initio* program for molecular electronic structure calculations written by H.-J. Werner and P. J. Knowles with contributions from a number of other people.
(34) Mebel, A. M.; Morokuma, K.; Lin, M. C. *J. Chem. Phys.* **1995**, *103*, 3440.
(35) Davigo, G. E.; Bierbaum, V.; DePuy, C. H.; Ellison, G. B.; Squires, R. S. *J. Am. Chem. Soc.* **1995**, *117*, 2590.
(36) Chase, M. W., Jr.; Davles, C. A.; Downey, J. R., Jr.; Frurip, D. J.; McDonald, R. A.; Syverud, A. N. JANAF Thermochemical Tables; *J. Phys. Chem. Ref. Data* **1985,** *14* (Suppl. 1).
(37) Ochterski, J. W.; Petersson, G. A.; Montgomery, Jr., J. A. *J. Chem. Phys.* **1996**, *104*, 2598.
(38) Knyazev, V. D.; Benscura, A., Stoliarov; S. I.; Slagle, I. R. *J. Phys. Chem.* **1996**, *100*, 11346.
(39) Logan, C. F.; Chen, P. *J. Am. Chem. Soc.* **1996**, *118*, 2113.
(40) Rauhut, G.; Pulay, P. *J. Phys. Chem.* **1995**, *99*, 3093.
(41) Radziszewski, J.; Nimlos, M. R.; Winter, P. R.; Ellison, G. B. *J. Am. Chem. Soc.* **1996**, *118*, 7400.
(42) Benson, S. W. *Thermochemical Kinetics: Methods for the Estimation of Thermochemical Data and Rate Parameters*, 2nd ed.; John Wiley: New York, 1976.
(43) Diau, E. W. G.; Lin, M. C. *J. Phys. Chem.* **1995**, *99*, 6589.
(44) Park, J.; Lin, M. C. *J. Phys. Chem. A* **1997**, *101*, 14.
(45) Park, J.; Dyakov, I. V.; Lin, M. C. Manuscript in preparation.
(46) Ackerman, L.; Hippler, H.; Pagsberg, P.; Reihs, C.; Troe, J. *J. Phys. Chem.* **1990**, *94*, 5247.
(47) Choudhury, T. K.; Sanders, W. A.; Lin, M. C. *J. Chem. Soc., Faraday Trans. 2* **1989**, *85*, 801.